ELSEVIER

Journal of Alloys and Compounds 363 (2004) 271–274

Journal of ALLOYS AND COMPOUNDS

www.elsevier.com/locate/jallcom

Synthesis of tin oxide nanoparticles by mechanochemical reaction

Huaming Yang*, Yuehua Hu, Aidong Tang, Shengming Jin, Guanzhou Qiu

Department of Inorganic Materials, School of Resources Processing and Bioengineering, Central South University, Changsha 410083, China

Received 23 February 2003; received in revised form 28 April 2003; accepted 28 April 2003

Abstract

The synthesis of tin oxide (SnO_2) nanoparticles by mechanochemical reaction ($SnCl_2 + Na_2CO_3$) with NaCl as diluent and subsequent thermal treatment was investigated using differential thermal analysis (DTA), thermogravimetric analysis (TGA), X-ray diffraction (XRD), infrared spectroscopy (IR) and transmission electron microscopy (TEM). Heat treatment of the as-milled powder at 600 °C in air and removal of NaCl through washing produced the SnO_2 nanocrystallites with an average crystal size of about 28 nm, varying with the thermal treatment temperature. The mechanism of nanocrystallites growth is discussed.

Keywords: Oxide materials; Nanostructured materials; Mechanochemical processing; X-Ray diffraction; TEM

1. Introduction

Tin oxide (SnO_2), a stable and large band-gap semiconductor, is one of the promising materials for gas sensors, optoelectronic devices and negative electrodes for lithium batteries [1–3]. However, its sensing and electrical properties are to a large degree influenced by many factors. Nanosized SnO_2 has especially good properties and has outstanding advantages of low operating temperature and high sensitivity for gas-sensing applications. The microstructure of the nanocrystallite depends on the preparation method. Many methods have been developed to synthesize SnO_2 nanoparticles, including low-temperature evaporation [4], homogeneous precipitation [5], water-in-oil microemulsions [6], microwave-assisted solution [7], sol–gel route [8–10], thermal decomposition [11], gas phase condensation [12], dual ion beam sputtering [13] and amorphous citrate route [14]. Nanocrystalline structures have been achieved by these techniques, but often with a very high degree of agglomeration.

Mechanochemical processing is a novel method for the production of nanosized materials, where separated nanoparticles can be prepared. The method has been widely applied to synthesize a large variety of nanoparticles, including ZnS, CdS, $LiMn_2O_4$, SiO_2 and CeO_2 [15–18]. Recently, a diluent, often the by-product of the reaction (salt), is added to the starting materials during the mechanochemical processing. It can separate the nanoparticles, prevent their subsequent growth, the synthesized powder being not significantly agglomerated. Removal of the salt matrix is usually carried out through simple washing [19]. Mechanochemical synthesis is a simple, cheap and convenient method suitable for large-scale production of nanoparticles. In this paper, the synthesis of SnO_2 nanoparticles by mechanochemical reaction of $SnCl_2$ with Na_2CO_3 is reported.

2. Experimental

The starting materials were AR-grade anhydrous $SnCl_2$, anhydrous Na_2CO_3 and NaCl. The NaCl was used as a diluent and added to the starting powder. A 30-g aliquot of sample, nine stainless steel balls of 2.5 mm diameter, and 40 stainless steel balls of 0.4 mm diameter were sealed in a 300-ml stainless steel vial using a ball to powder mass ratio of 10:1. Mechanochemical milling was carried out with a KM-10 type planetary mill for 4 h at 600 rpm. The as-milled powder was then annealed at 600 °C in air and the by-product NaCl was removed through washing with distilled water in an ultrasonic bath. The SnO_2 nanoparticles were obtained from the drying of the washed powders.

Simultaneous TGA–DTA of the as-milled powder was carried out using an SDT2960 thermal analysis system at a

* Corresponding author. Tel.: +86-731-883-0549; fax: +86-731-871-0804.
E-mail address: hmyang@mail.csu.edu.cn (H. Yang).

0925-8388/$ – see front matter © 2003 Elsevier B.V. All rights reserved.
doi:10.1016/S0925-8388(03)00473-0

heating rate of 20 °C/min. The structure of the nanoparticle was examined using a D/max-γA diffractometer (Cu Kα radiation, λ = 0.154056 nm) and an AVATAR-360 infrared (IR) instrument. The nanoparticle morphology was examined in a JEM-200CX transmission electron microscope. The average crystal size (*D*) of the nanoparticle was evaluated from Scherrer's equation.

3. Results and discussion

A stoichiometric mixture of the starting materials was milled corresponding to the following reaction equation

$$SnCl_2 + Na_2CO_3 + 6NaCl = SnO + CO_2 + 8NaCl \quad (1)$$

Fig. 1 shows the XRD patterns of: (a) the starting materials, (b) powders milled for 4 h, (c) after subsequent heat treatment at 600 °C, (d) after washing. Only the peaks of the three starting materials were observed in the patterns of the as-mixed powder (a). After milling for 4 h, the pattern shows the peaks of SnO and NaCl phases with no trace of $SnCl_2$ and Na_2CO_3. This is indicative of the occurrence of the solid-state displacement reaction (1) in a stable-state manner. A new peak associated with SnO_2 was observed in the pattern of the sample after thermal treatment of the as-milled powder. After washing, only those peaks coincident with SnO_2 remained, indicating the complete removal of the NaCl by-product phase.

Fig. 2 shows the TGA–DTA curves of the powder washed after 4 h milling which includes only the SnO phase. An evident exothermal peak resulting from oxidization was observed at approximately 400–550 °C. The TGA curve exhibits an apparent increase in sample weight from ambient to 600 °C. The weight increase of 11.64% agrees well with the theoretical value 11.88% associated with the following chemical reaction

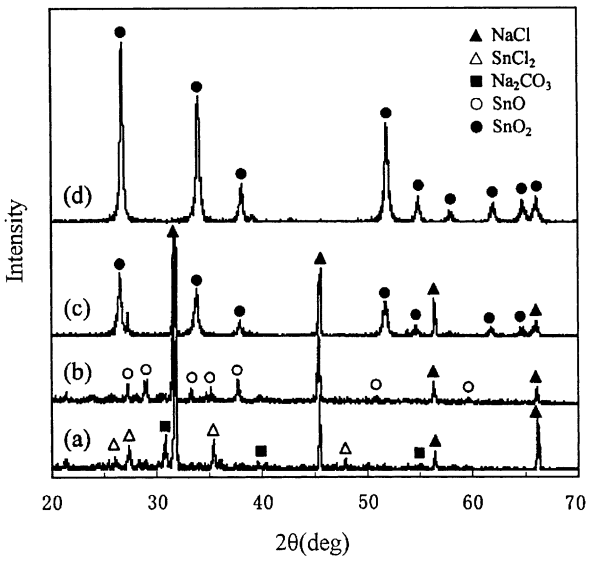

Fig. 1. XRD patterns of the $SnCl_2 + Na_2CO_3 + 6NaCl$ powder mixture; (a) the starting materials, (b) the as-milled materials (milled for 4 h), (c) after calcination at 600 °C for 2 h, and (d) when washed after calcination.

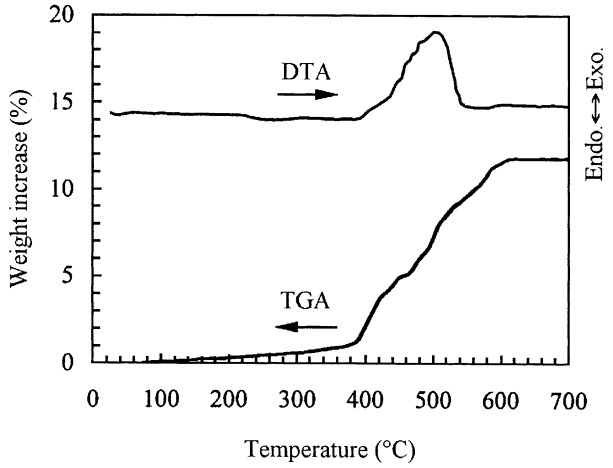

Fig. 2. TGA–DTA curves of the as-milled powder after washing.

$$SnO + 1/2O_2 = SnO_2 \quad (2)$$

The present result is very close to results reported elsewhere. Ramamoorthy et al. reported that transformation of SnO into SnO_2 occurs at 500–600 °C during heating either directly or by passing an intermediate phase [20]. Moreover, the results of Kobayashi et al. also indicated that the SnO grown by heating at 450–500 °C can change to SnO_2 [21].

Fig. 3 shows the XRD patterns of the SnO_2 nanoparticles synthesized at 500–800 °C. Due to the increase in the calcination temperature, the intensities of the peaks associated with SnO_2 increased to some extent. From the corresponding IR spectra shown in Fig. 4, the band at 621 cm^{-1} was

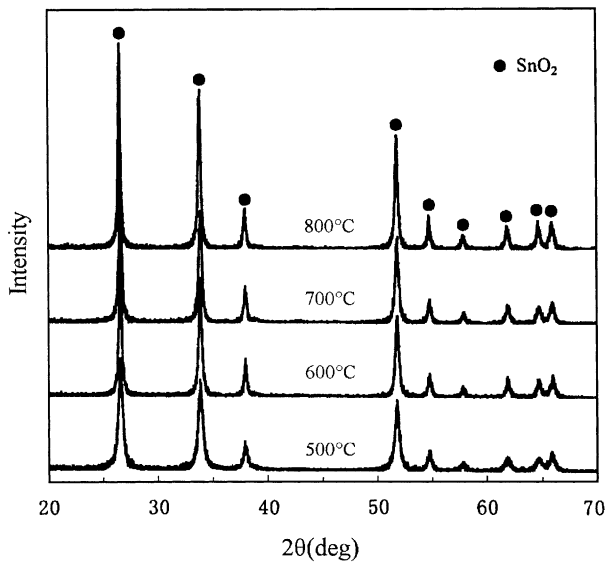

Fig. 3. XRD patterns of the SnO_2 nanoparticles synthesized at different calcination temperatures.

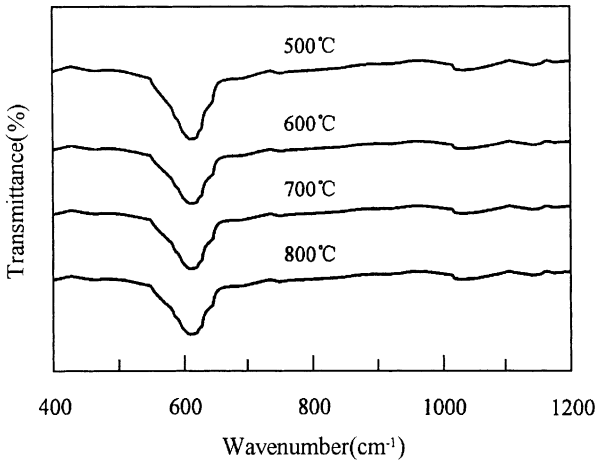

Fig. 4. FT-IR spectra of the SnO_2 nanoparticles synthesized at different calcination temperatures.

attributed to the Sn–O lattice vibration and became broadened with increasing calcination temperature.

Fig. 5 shows a plot of the SnO_2 XRD crystal size (D) as a function of heat treatment temperature for the as-milled powder. The crystal size increased slowly from about 25 nm at 450 °C to 28 nm at 600 °C and then increased rapidly above 650 °C. The D value reached 40 nm at 800 °C calcination. This is directly related to the crystallization of nanoparticles.

Fig. 6 shows a TEM micrograph of the SnO_2 nanoparticles when washed after heat treatment at 600 °C. The particle size is in good agreement with the XRD evaluation. Moderately agglomerated particles appear to be present.

Straight lines of ln(D) against 1/T are plotted in Fig. 7 according to the Scott equation given below on the assumption that the nanocrystallite growth is homogeneous [22], which approximately describes the nanocrystallite growth during annealing:

$$D = C\exp(-E/RT) \quad (3)$$

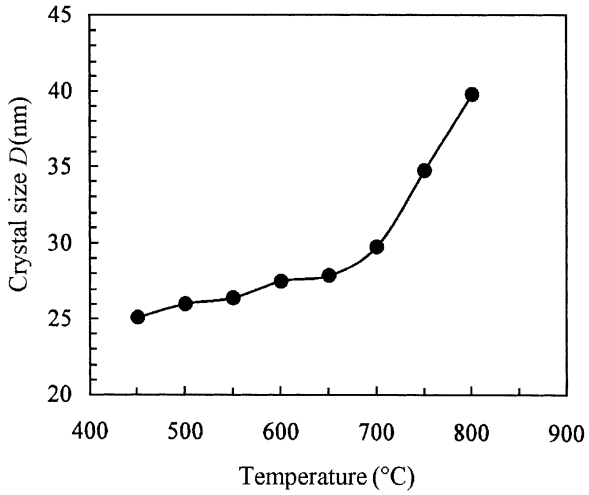

Fig. 5. Effect of calcination temperature on the average crystal size (D) of SnO_2 nanoparticles.

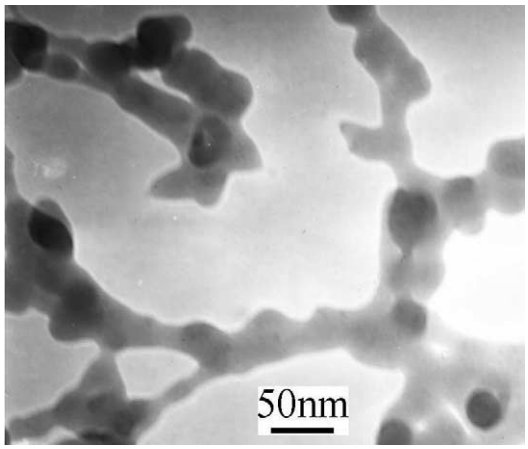

Fig. 6. TEM micrograph of the SnO_2 nanoparticles.

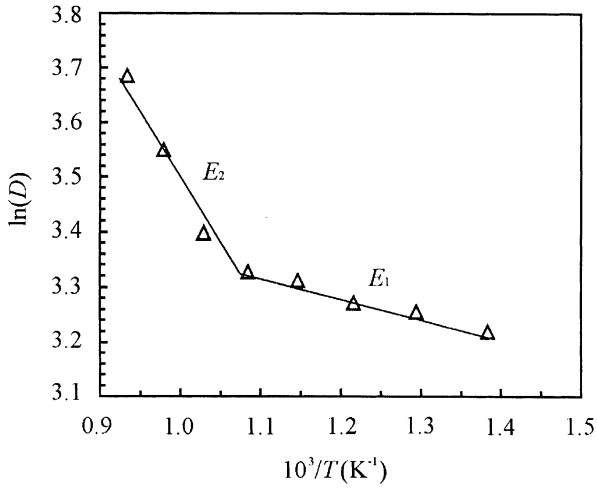

Fig. 7. Plot of ln(D) against 1/T for the equation $D = C\exp(-E/RT)$.

where D is the XRD average crystal size, C is a constant, E is the activation energy for nanocrystallite growth, R is the ideal gas constant and T is the absolute temperature.

Two straight lines exist for different temperatures and 650 °C can be regarded as a critical temperature. It indicates that the nanocrystallite grows in different ways. In the range below 650 °C for thermal treatment, the calculated value of the activation energy (E_1) is 35.8 kJ/mol. It can be considered that the crystallite grows primarily by means of an interfacial reaction. On the other hand, the higher activation energy ($E_2 = 237.5$ kJ/mol) above 650 °C indicates that the crystallite grows more quickly by means of grain boundary shift. The crystal size becomes larger and increases rapidly with increasing temperature, as can be confirmed from Fig. 5.

4. Conclusions

Tin oxide (SnO_2) nanoparticles can be successfully synthesized by heat treatment of as-milled powder obtained by

mechanochemical reaction of $SnCl_2$ and Na_2CO_3 with NaCl as a diluent. The XRD crystal size of the SnO_2 nanoparticle gradually increased with increasing heat treatment temperature, the particle size ranging from 25 to 40 nm at 450–800 °C. This route is also applicable to the synthesis of other functional nanoparticles. The calculation of the activation energy indicates that the nanocrystallite growth involves a complex chemical process and different mechanisms exist at different calcination temperatures.

Acknowledgements

This work was supported by the National Science Foundation for Distinguished Young Scholar of China (No. 59925412) and the Excellent Doctoral Dissertation Foundation of Hunan Province (No. 200114).

References

[1] A.C. Bose, D. Kalpana, P. Thangadurai, S. Ramasamy, J. Power Sources 107 (2002) 138–141.
[2] F. Belliard, P.A. Connor, J.T.S. Irvine, Solid State Ionics 135 (2000) 163–167.
[3] F. Lu, Y. Liu, M. Dong, X. Wang, Sensors Actuators B 66 (2000) 225–227.
[4] Y. Chen, X. Cui, K. Zhang, D. Pan, Chem. Phys. Lett. 369 (2003) 16–20.
[5] K.C. Song, Y. Kang, Mater. Lett. 42 (2000) 283–289.
[6] K.C. Song, J.H. Kim, Powder Technol. 107 (2000) 268–272.
[7] D.S. Wu, C.Y. Han, S.Y. Wang, N.L. Wu, Mater. Lett. 53 (2002) 155–159.
[8] R. Pella, Sensors Actuators B 44 (1997) 462–467.
[9] A. Wilson, Sensors Actuators B 18/19 (1994) 506–510.
[10] H. Shiomi, C. Kakimoto, A. Nakakira, J. Sol-Gel Sci. Technol. 19 (2000) 759–763.
[11] C. Xu, G. Xu, Y. Liu, X. Zhao, Scripta Mater. 46 (2002) 789–794.
[12] J.-M. Herrmann, J. Disdier, A. Fernández, V.M. Jiménez, Nanostruct. Mater. 8 (1997) 675–686.
[13] Y.C. Choe, J.H. Chung, D.S. Kim, H.K. Baik, Surf. Coat. Technol. 112 (1999) 267–270.
[14] M. Bhagwat, P. Shah, V. Ramaswamy, Mater. Lett. 57 (2003) 1604–1611.
[15] P. Baláž, E. Boldižárová, E. Godočíková, J. Briančin, Mater. Lett. 57 (2003) 1585–1589.
[16] F. Li, X. Yu, H. Pan, M. Wang, X. Xin, Solid State Sci. 2 (2000) 767–772.
[17] S. Soiron, A. Rougier, L. Aymard, J.-M. Tarascon, J. Power Sources 97/98 (2001) 402–405.
[18] Q. Zhang, F. Saito, J. Alloys Comp. 297 (2000) 99–103.
[19] Ü. Kersen, Appl. Phys. A 75 (2002) 559–563.
[20] R. Ramamoorthy, M.K. Kennedy, H. Nienhaus, Sensors Actuators B 88 (2002) 281–285.
[21] T. Kobayashi, Y. Kimura, H. Suzuki, J. Cryst. Growth 243 (2002) 143–150.
[22] M.G. Scott, Amorphous Metallic Alloys Butterworths, London, 1983, p. 151.